Search for a New Neutral Boson in the Rare Decay $K_L \to \pi^0\pi^0\mu^+\mu^-$

D.G. PHILLIPS II, on behalf of the KTeV Collaboration

Department of Physics, University of Virginia

382 McCormick Road, Charlottesville, Virginia 22904 USA

email: dgp6d@virginia.edu

Using data collected by the KTeV Experiment at Fermi National Accelerator Laboratory in Batavia, Illinois, this study will be the first experimental analysis of $K_L \to \pi^0\pi^0\mu^+\mu^-$. Although this decay mode is possible within the Standard Model, it is limited to a very narrow band of phase space. The HyperCP Experiment has recently observed three $\Sigma^+ \to p\mu^+\mu^-$ events within a narrow dimuon mass range of 213.8 MeV/c^2 to 214.8 MeV/c^2. This suggests that the process could occur via a neutral intermediary particle, $\Sigma^+ \to pX^0 \to p\mu^+\mu^-$, with an X^0 mass of 214.3 MeV/$c^2$$\pm$0.5 MeV/$c^2$. Since the X^0 has a light mass and a low interaction probability, then it is most likely a new neutral boson outside the Standard Model. Recent theoretical predictions suggest that the decay mode $K_L \to \pi^0\pi^0\mu^+\mu^-$ can also occur via the aforementioned neutral boson: $K_L \to \pi^0\pi^0X^0 \to \pi^0\pi^0\mu^+\mu^-$. Therefore, in addition to a measurement of the Standard Model process whereby an intermediate photon goes to $\mu^+\mu^-$, the search for $K_L \to \pi^0\pi^0\mu^+\mu^-$ is also carried out in an effort to address the viability of X^0 in explaining the HyperCP phenomena.

1 Introduction

In this report, we present the first attempt to detect the rare decay modes $K_L \to \pi^0\pi^0\mu^+\mu^-$ and $K_L \to \pi^0\pi^0X^0 \to \pi^0\pi^0\mu^+\mu^-$. Based on an observation of three events in a study of the decay $\Sigma^+ \to p\mu^+\mu^-$, the HyperCP collaboration reported the possible observation of an X^0 boson of mass 214.3 MeV/c^2 decaying into a $\mu^+\mu^-$ [1]. The aforementioned results from the HyperCP experiment provide the incentive to search for the decay $K_L \to \pi^0\pi^0X^0 \to \pi^0\pi^0\mu^+\mu^-$.

Using a model in which the X^0 couples to the $\bar{d}s$ and the $\mu^+\mu^-$, theoretical estimates of the $K_L \to \pi^0\pi^0X^0 \to \pi^0\pi^0\mu^+\mu^-$ branching ratio were determined to be $(8.3^{+7.5}_{-6.6})\times10^{-9}$ for a pseudoscalar X^0 and $(1.0^{+0.9}_{-0.8})\times10^{-10}$ for a axial vector X^0 [2]. In this model, the scalar and vector X^0 were ruled out as explanations for the HyperCP hypothesis of the X^0 particle. Another model predicts a branching ratio for $K_L \to \pi^0\pi^0X^0 \to \pi^0\pi^0\mu^+\mu^-$ of 8.02×10^{-9} for a neutral spin zero pseudoscalar boson X^0 [3]. An alternate model proposes the light pseudoscalar Higgs boson from the next-to-minimal supersymmetric standard model (NMSSM) as an explanation of the HyperCP result [4]. There is currently no prediction for the branching ratio of $K_L \to \pi^0\pi^0 X^0 \to \pi^0\pi^0\mu^+\mu^-$ using NMSSM. A theoretical study on the rare decay $K_L \to \pi^0\pi^0\mu^+\mu^-$ has not yet been performed within the framework of the standard model.

1.1 Description of the Experiment

The search for the $K_L \to \pi^0\pi^0\mu^+\mu^-$ mode was performed by analyzing data from the 1997 and 1999 runs of KTeV E799 II at Fermi National Accelerator Laboratory. The KTeV E799 experiment produced neutral kaons via collisions of 800 GeV/c protons with a BeO target. The particles created from interactions with the target passed through a series of collimators, absorbers and sweeper magnets to produce two nearly parallel K_L beams. The K_L beams then entered a 70 m long vacuum tank, which was evacuated to 1 μTorr. Immediately downstream of the vacuum region was a spectrometer, which was composed of an analysis magnet sandwiched between two pairs of drift chambers. These were followed by transition radiation detectors and two planes of trigger hodoscopes.

The two vital elements to this analysis were the CsI electromagnetic calorimeter and the muon ID system, which were located at 186.0 m and 188.5 m from the BeO target respectively. Constructed of 3100 CsI crystal blocks arranged into a (1.9×1.9) m array, the CsI calorimeter was used as another tool for charged particle discrimination through measurement of the quantity E/p. E is the energy of the cluster associated with the track and p is the momentum of the same track. Each crystal was 27 radiation lengths (1.4 nuclear interaction lengths) long. Two holes are located near the center of the calorimeter to allow for passage of the neutral beams. The muon ID system was composed of a lead wall, three particle filters and three scintillator counter planes designed to identify muons by filtering out other charged particles. In total, the lead wall and three filters amounted to 31 nuclear interaction lengths of material. Figure 1 shows a cross-sectional view of the KTeV detector and vacuum decay region. A more detailed description of the KTeV detector can be found in [5, 6].

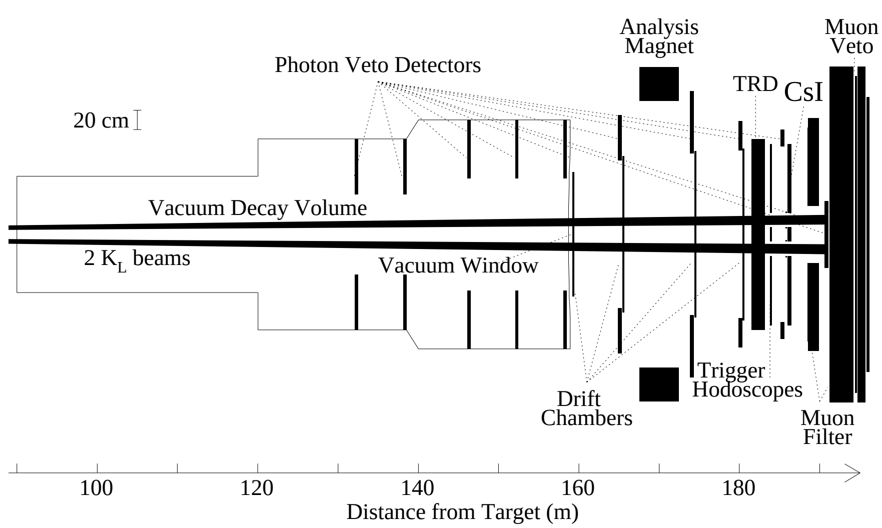

Figure 1: Top view of the KTeV detector and vacuum decay region in the E799 configuration.

1.2 1997 and 1999 Run Periods

The 1997 and 1999 runs differed in the following ways. The spill length was doubled from 20 seconds in the 1997 run to 40 seconds in the 1999 run. The proton intensity on the BeO neutral kaon production target was increased from $2-4\times10^{12}$ protons per spill in the 1997 run to $6-10\times10^{12}$ protons per spill in the 1999 run. Another important difference between the 1997 and 1999 run was the magnetic field in the spectrometer. In the 1997 run, the magnetic field elicited a momentum kick of 205 MeV/c to charged particles in x-z plane of the spectrometer. In the 1999 run, the magnetic field was changed to yield a momentum kick of 150 MeV/c in the x-z plane to increase acceptance for select neutral kaon modes.

1.3 Signal and Normalization Mode Triggers

The signal modes and normalization mode were located on different triggers. Both signal modes used $K_L\to\pi^0\pi^0\pi^0_D$ as the common normalization mode, where one of the π^0s undergoes the dalitz decay $\pi^0_D\to e^+e^-\gamma$. The normalization mode was chosen due to its high branching ratio and due to the lack of any heretofore observed neutral K_L decay modes with two tracks and four photons. The signal mode trigger was changed in the 1999 run to allow for one missing hit in either the x or y view of the last set of muon ID system counting planes. In order to counteract this effect, the number of hardware clusters was increased from a minimum of one to two for the 1999 run. The normalization mode trigger which demanded two charged tracks and at least four electromagnetic clusters was loosened midway through the 1997 run by changing the minimum thresholds for energy in the electromagnetic calorimeter. These changes to the minimum thresholds were kept intact for the 1999 run.

2 Signal Mode Analysis

The $K_L\to\pi^0\pi^0\mu^+\mu^-$ and $K_L\to\pi^0\pi^0X^0\to\pi^0\pi^0\mu^+\mu^-$ final states are composed of four photons plus a $\mu^+\mu^-$. The difference between these two final states is that the former and latter are considered as a four-body and three-body decay respectively. The presence of four photons and lack of phase space available to the signal modes forces the vast majority of all possible backgrounds to the high $M_{\mu\mu\gamma\gamma\gamma\gamma}$ region. This allowed for background issues to be effectively addressed with a loose set of cuts, which also yielded good signal acceptance.

2.1 Analysis Cuts

Both charged tracks were obligated to form a good vertex within the vacuum decay region, to match a cluster in the CsI calorimeter, to have $E/p\le0.9$ and deposit less than 1 GeV of energy in the CsI calorimeter. In addition, the track momentum was limited to values greater than 7.0 GeV/c. The latter three requirements are consistent with minimum ionizing muons. Each of the final three counting planes in the muon ID system were required to log at least one hit. A loose requirement on the invariant dimuon mass, $M_{\mu\mu}\le232$ MeV/c^2, was also implemented.

The number of clusters in the CsI calorimeter not associated with tracks was required to be equal to four. These clusters were directly coupled to the two π^0s from the signal modes. Due to the narrow opening angle of the dimuon vertex, the z vertex was determined using a neutral vertex calculated from the two $\gamma\gamma$ vertices associated the $\pi^0\pi^0$. Reconstruction of the $\pi^0\pi^0$ was performed by analyzing each possible $\gamma\gamma$ pair in order to find the combination with the best agreement of the position of two neutral vertices determined from each pair of photons under the hypothesis that they originated in a π^0 decay. The z-vertex for the event is then calculated as a weighted average of z-vertex values for each $\gamma\gamma$ in the π^0 pairing with the minimum pairing chi-squared of the z-vertex. This z-vertex was required to lie within the range of 90 m to 160 m from the target, which encompasses the full length of the vacuum decay region. Each $\gamma\gamma$ mass in a given event, $M_{\gamma\gamma}$, is extracted as a byproduct of the neutral z-vertexing procedure and was required to be within 9 MeV/c^2 of the π^0 mass. Further details can be found in [7].

2.2 Discussion of Backgrounds

Any K_L decay mode with two minimum ionizing tracks and at least one photon was generated with the Monte Carlo (MC) and analyzed as a potential source of background. If the minimum ionizing track was a $\pi^{\pm}$, then cases of both pion punch through to the muon ID system and pion decay were generated in the MC and analyzed as separate sources of background. All K_L decay mode backgrounds in these scenarios are missing a minimum of two photons needed to reconstruct the signal mode topology. Aside from mismeasurements, accidental photons are employed in the MC to fill this void, which forces $M_{\mu\mu\gamma\gamma\gamma\gamma}$ into a region above the K_L mass. Approximately eleven billion background events were generated in the MC. After all signal mode analysis cuts there were zero background events remaining in the masked signal regions.

2.3 Masked Signal Boxes

The signal regions for the 1997 and 1999 data were based on the $M_{\mu\mu\gamma\gamma\gamma\gamma}$, $p_T^2(\mu\mu\gamma\gamma\gamma\gamma)$ and $|p^2_{T,\mu\mu} - p^2_{T,\pi\pi}|$ resolutions calculated using two signal mode MCs. Here p_T^2 is measured relative to the direction of the K_L determined by the line connecting the BeO target center and the decay vertex. For the 1997 and 1999 data, the masked signal region for the K_L decay was chosen to be rectangular with 0.495 GeV/c^2 $\leq M_{\mu\mu\gamma\gamma\gamma\gamma} \leq$ 0.501 GeV/c^2 and $p_T^2 \leq 0.00013$ (GeV/c)^2. This region shall henceforward be referred to as the first masked signal box. In both data sets, the masked signal region for the X^0 decay was chosen to be rectangular with 213.8 MeV/c^2 $\leq M_{\mu\mu} \leq$ 214.8 MeV/c^2 and $|p^2_{T,\mu\mu} - p^2_{T,\pi\pi}| \leq 0.0007$ (GeV/c)^2. The immediately aforementioned region shall henceforward be referred to as the second masked signal box. The constraint on $M_{\mu\mu}$ was chosen based on the predicted X^0 mass made by the HyperCP collaboration [1]. Figure 2 shows p_T^2 vs. invariant mass scatter plots of the $K_L \rightarrow \pi^0\pi^0\mu^+\mu^-$ and $K_L \rightarrow \pi^0\pi^0 X^0 \rightarrow \pi^0\pi^0\mu^+\mu^-$ signal mode MC respectively. Generation of the signal mode MC with accidental photons led to some mismeasured events, which were pushed outside the signal mode region as a result.

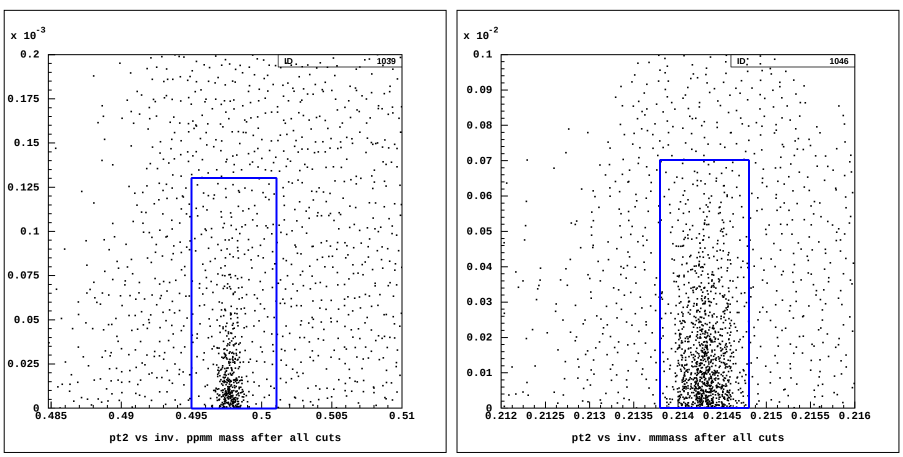

Figure 2: On the left is the p_T^2 vs. $M_{\mu\mu\gamma\gamma\gamma\gamma}$ scatter plot for the 1997 $K_L \rightarrow \pi^0\pi^0\mu^+\mu^-$ MC. On the right is the $|p^2_{T,\mu\mu} - p^2_{T,\pi\pi}|$ vs. $M_{\mu\mu}$ scatter plot for the 1997 $K_L \rightarrow \pi^0\pi^0 X^0 \rightarrow \pi^0\pi^0\mu^+\mu^-$ MC. Both plots are shown immediately after all analysis requirements were applied. The blue boxes indicate the locations of the masked signal boxes, which are open in the MC.

3 Normalization Mode Analysis

The normalization mode chosen for this analysis was $K_L \rightarrow \pi^0\pi^0\pi^0_D$, where $\pi^0_D \rightarrow e^+e^-\gamma$. The presence of an extra photon and two electrons instead of two muons are the only differences between the normalization mode and the signal modes. As in the signal mode, the four photons

Source of Systematic Error on F_K	$\frac{\Delta F_K(1997)}{F_K(1997)}$	$\frac{\Delta F_K(1999)}{F_K(1999)}$
Variation of Kinematic Requirements	+1.26%	+2.24%
p_z Weighting	—	1.87%
Cracks in Muon Counting Planes	0.50%	0.50%
Energy Loss in Muon Filters	0.40%	0.40%
$BR(K_L \to \pi^0\pi^0\pi^0)$	0.61%	0.61%
Total Systematic Error	+1.54%	+3.05%

Table 1: Summary of systematic errors on the K_L flux, labeled as F_K.

which gave the minimum pairing chi-squared of the z-vertex were associated with the π^0 pair for that event. The remaining photon was partnered with the π^0_D state. The z-vertex in the normalization mode analysis was chosen to be 94 m to 158 m from the target.

3.1 Backgrounds to the Normalization Mode

The only noticeable background to the normalization mode was when a photon from $K_L \to \pi^0\pi^0\pi^0$ underwent pair production in the vacuum window or detector material upstream of the first drift chamber. Only very loose cuts on the normalization mode invariant mass ($M_{ee\gamma\gamma\gamma\gamma}$), p_T^2 and $M_{\gamma\gamma}$ were needed to extract the normalization mode signal and sweep away the photon conversion background. $M_{ee\gamma\gamma\gamma\gamma}$ was required to reside between 473 MeV/c^2 and 523 MeV^2, while $p_T^2 \leq 0.001$ GeV^2/c^2 and $M_{\gamma\gamma}$ was situated within 14 MeV/c^2 of the π^0 mass. After generating approximately two fluxes of $K_L \to \pi^0\pi^0\pi^0$ events in MC (where one of the photons underwent photon conversion), only one $K_L \to \pi^0\pi^0\pi^0$ MC event was found after all analysis requirements were implemented. This was negligible compared to the number of events found in the data after all analysis requirements were applied. Therefore, backgrounds did not have a noticeable effect on the K_L flux.

4 Uncertainties in the Flux

Uncertainties in the K_L flux originated from the branching ratio used to calculate the flux, uncertainty in the placement of kinematical analysis requirements, the resolution of the total z momentum, p_Z, and the efficiency of the muon ID system. The statistical errors on the signal mode MC were less than 0.14% for each decay mode, while the statistical error for both the normalization mode data and MC was less than 0.31%. All systematic errors in this analysis came from the normalization mode. The total uncertainty due to kinematical analysis requirements was determined by varying the z-vertex, $M_{ee\gamma\gamma\gamma\gamma}$, p_T^2, $M_{\gamma\gamma}$ and E/p. The uncertainty from p_Z was calculated by applying a set of weights to flatten the data/MC ratio of the p_Z spectrum. Systematic errors in the muon ID efficiency stemmed from modeling of the energy loss in the muon filters and from simulation of gaps between scintillator paddles in the last two muon counting planes [8]. Results from these systematic error studies are given in Table 1.

5 Calculation of the Upper Limit

The 1997 (1999) signal mode acceptance was 3.14% (4.03%) and 2.80% (3.74%) for $K_L \to \pi^0\pi^0\mu^+\mu^-$ and $K_L \to \pi^0\pi^0X^0 \to \pi^0\pi^0\mu^+\mu^-$ respectively. The total K_L flux was calculated as the summation of the 1997 and 1999 K_L fluxes and was found to be 7.33 $\times 10^{11}$. This flux resulted in a single event senitivity of 3.75 $\times 10^{-11}$ for $K_L \to \pi^0\pi^0\mu^+\mu^-$ and 4.10 $\times 10^{-11}$ for $K_L \to \pi^0\pi^0X^0 \to \pi^0\pi^0\mu^+\mu^-$. As displayed in figure 3, no events were found inside the signal regions upon opening the masked signal boxes. This yielded 90% confidence level upper limits of $BR(K_L \to \pi^0\pi^0\mu^+\mu^-) < 8.63 \times 10^{-11}$ and $BR(K_L \to \pi^0\pi^0 X^0 \to \pi^0\pi^0\mu^+\mu^-) < 9.44 \times 10^{-11}$ using the methodology adopted in [9], which holds for either a Bayesian or Classical viewpoint.

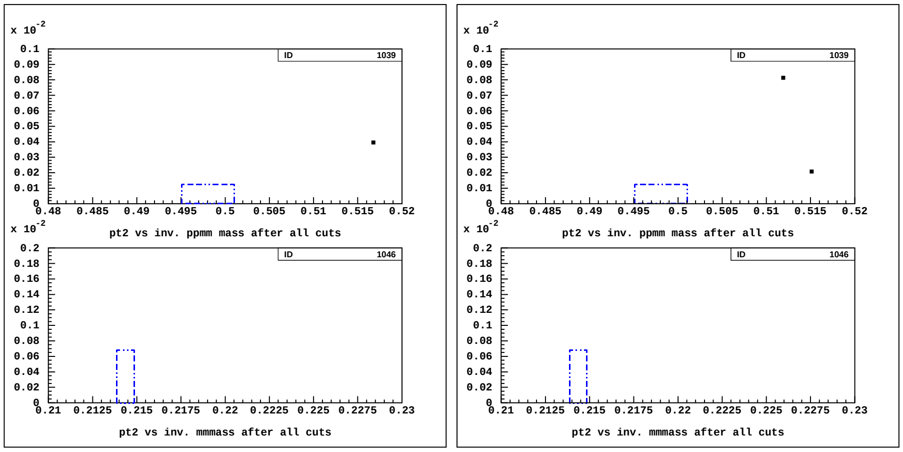

Figure 3: On the left is the p_T^2 vs. $M_{\mu\mu\gamma\gamma\gamma\gamma}$ scatter plot for the 1997 data set (top) and the $|p^2_{T,\mu\mu} - p^2_{T,\pi\pi}|$ vs. $M_{\mu\mu}$ scatter plot for the 1997 data set (bottom). On the right is the p_T^2 vs. $M_{\mu\mu\gamma\gamma\gamma\gamma}$ scatter plot for the 1999 data set (top) and the $|p^2_{T,\mu\mu} - p^2_{T,\pi\pi}|$ vs. $M_{\mu\mu}$ scatter plot for the 1999 data set (bottom). Both plots are shown immediately after the masked signal boxes were opened, which are indicated by dotted blue boxes.

6 Conclusion

This letter presents the first experimental study of the decay modes $K_L \to \pi^0\pi^0\mu^+\mu^-$ and $K_L \to \pi^0\pi^0X^0 \to \pi^0\pi^0\mu^+\mu^-$. Our result for $BR(K_L \to \pi^0\pi^0X^0 \to \pi^0\pi^0\mu^+\mu^-)$ is 88 times smaller than the expected branching ratio with a pseudoscalar X^0 from [2] and 85 times smaller than the expected branching ratio with a pseudoscalar X^0 from [3]. In addition, our result was found to be within the bounds of the theoretical branching ratio of $K_L \to \pi^0\pi^0X^0 \to \pi^0\pi^0\mu^+\mu^-$ from [2] with an axial vector X^0. This effectively rules out the pseudoscalar X^0 as an explanation of the HyperCP result.

Acknowledgments

We thank the Fermi National Accelerator Laboratory staff for their contributions. This work was supported by the U.S. Department of Energy, the U.S. National Science Foundation, the Ministry of Education and Science of Japan, the Fundao de Amparo a Pesquisa do Estado de Sao Paulo-FAPESP, the Conselho Nacional de Desenvolvimento Cientifico e Tecnologico-CNPq, and the CAPES-Ministerio da Educao.

References

1. H.K. Park *et al.* (HyperCP Collaboration), *Phys. Rev. Lett.* **94**, 021801 (2005)
2. X.-G. He, J. Tandean, and G. Valencia, *Phys. Lett.* B **631**, 100 (2005).
3. N.G. Deshpande, G. Eilam, and J.Jiang, *Phys. Lett.* B **632**, 212 (2006).
4. X.-G. He, J. Tandean, and G. Valencia, *Phys. Rev. Lett.* **98**, 081802 (2007).
5. A. Alavi-Harati *et al.*, *Phys. Rev.* D **67**, 012005 (2003).
6. C. Bown *et al.*, *Nucl. Instrum. Methods* A **369**, 248 (1996).
7. D.G. Phillips II, *PhD Thesis*, Univ. of Virginia (2009).
8. B. Quinn, *PhD Thesis*, Univ. of Chicago (2000).
9. R.D. Cousins and V.L. Highland, *Nucl. Instrum. Methods* A **320**, 331 (1992).